1st INTERNATIONAL CONFERENCE ON
Climate Change & Sustainable Development
"Shaping a Sustainable Future: Global Solutions for Climate Change"
25th to 26th Feb 2025
SINES, NUST Islamabad

Numerical Analysis on Drag-based Wind Turbines for Optimal Tip-speed Ratio

Hamza Latif Mehr[1], Imran Akhtar[2]

[1]*Department of Mechanical Engineering, National University of Sciences & Technology (NUST) CEME, hamzamehr.hm@gmail.com*

[2]*School of Interdisciplinary Engineering and Sciences (SINES), National University of Sciences & Technology (NUST)*

Abstract

Drag-based Vertical-Axis Wind Turbines (VAWTs), such as the Savonius type, present a practical solution for small-scale renewable energy needs due to their simple structure and ability to perform well in low wind conditions. This study examines the optimal tip-speed ratio (TSR) for Savonius turbines using computational fluid dynamics (CFD) simulations across various TSR values. The simulation results are validated against publicly available experimental data from Sandia National Laboratories, USA. The research analyzes key aerodynamic characteristics of the Savonius rotor, focusing on flow separation and the role of 2D CFD model accuracy in achieving reliable validation. It also explores how different TSRs influence wake behavior and turbine performance. The results highlight the importance of selecting an optimal TSR to improve efficiency and stabilize the wake flow. Furthermore, the study compares the aerodynamic performance of drag-based Savonius turbines with that of lift-based Darrieus turbines. Potential future work includes leveraging optimization algorithms to explore the design space, aiming to refine TSR values and enhance turbine geometry using advanced design strategies.

Keywords: *Vertical-Axis Wind Turbine, Savonius, Darrieus, Wake Analysis, Tip-Speed Ratio, torque coefficient, power coefficient*

1. INTRODUCTION

In response to the challenges posed by global warming, the depletion of fossil fuel reserves, and stricter environmental restrictions in the global energy market and society, the usage of renewable energy sources has grown dramatically during the past ten years [1] with wind energy leading the renewables. Wind turbines are primarily classified based on how they capture wind energy and convert it into

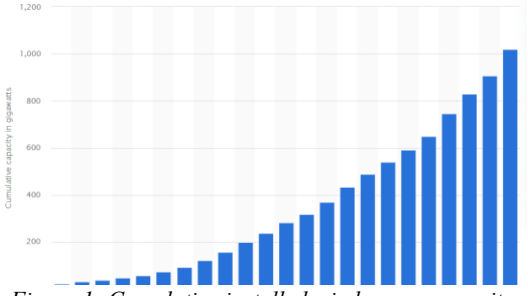

Figure 1: Cumulative installed wind power capacity worldwide from 2001 to 2023 [4]

mechanical energy. This classification is fundamentally determined by the turbine's structure or design, leading to a clear distinction between two types: Horizontal-axis wind turbines (HAWT), where the rotation axis is

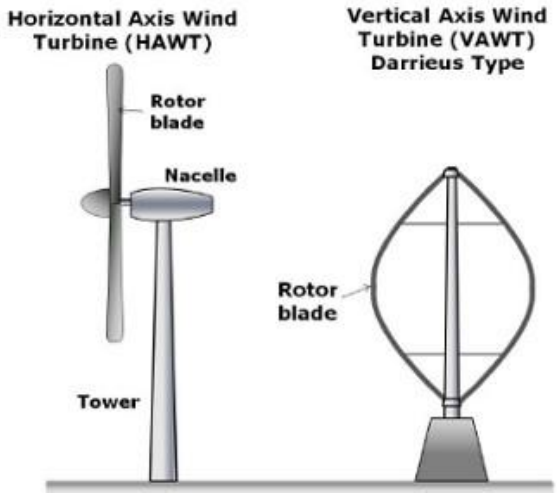

Figure 2: Horizontal and Vertical Axis Wind Turbine [2]

horizontal, and Vertical-axis wind turbines (VAWT), where the rotation axis is vertical. As shown in Figure 2 [2]. There are many different types of VAWT geometries based on their working principle i.e., lift or drag, as shown in Figure 3 [3]. Lift-based VAWTs include Darrieus turbines with curved blades, H-rotors with straight blades for easier maintenance, and helical designs with twisted blades that improve self-starting, reduce torque ripple, and enhance stability. Although VAWTs are cheap but the fundamental issue in VAWT is its limitation in power output. The output of VAWT can be measured by the coefficient of power (Cp).

A VAWT's performance curve reveals key efficiency metrics like the optimal TSR (λopt) and maximum power coefficient. At λopt, blades operate under ideal flow, maximizing energy extraction. Beyond this point, efficiency

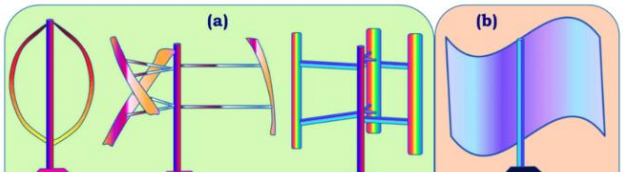

Figure 3 Lift type and Drag type HAWT [3]

drops due to flow blockage around the turbine. The design parameters that affect the performance of a VAWT are shown in Figure 4 [4].

Extensive studies on performance parameters of VAWTs cane be found in the literature. In one such study, Hand [4] analyzed VAWT blade configurations, recommending two blades for higher efficiency and stiffness, and three for better self-starting and lower torque ripple; also emphasizing minimizing drag losses at high TSR using streamlined struts and fairings. To measure the performance parameters, it has become increasingly important to develop techniques other than inexpensive experimental techniques, such as CFD. It plays a crucial role in blade analysis, design, and optimization, with various aspects highlighted across review studies in VAWTs [5], which are discussed in the following sections.

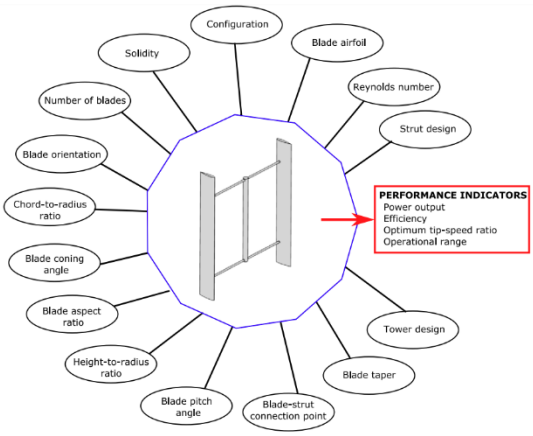

Figure 4: Performance Parameters of Wind Turbine [4]

CFD in VAWTs

CFD simulations offer a reliable approach for evaluating turbine efficiency, yet they come with trade-offs between computational cost and accuracy. Maican and Biriş [5] showed that while 2D simulations offer preliminary insights, they often overestimate torque due to missing 3D vortex effects, making 3D modeling essential for accurate results. However, turbulence models

like k-ε with enhanced wall treatment were not compared with k-ω, limiting the analysis.

Traditional Savonius turbines rely primarily on drag forces, limiting their efficiency. Ferrari et al. [6] compared 2D and 3D models of a Savonius VAWT, finding that 2D simulations overestimated efficiency by up to 20%, while 3D models aligned better with experiments, reaching a Cp of 0.202 at TSR 0.8. Though effective, the method was computationally expensive, and only one turbulence model with acceptable y^+ was used. More robust models like k-ε EWT, which are nearly y^+-independent, were not explored, limiting the turbulence analysis. Dewan et al. [7] reviewed CFD studies on Savonius turbines, emphasizing the influence of design parameters and turbulence models. They noted the widespread use of RANS models for their low cost but highlighted the challenge of selecting accurate models—a key limitation, as more advanced models remain underexplored. Heydari et al. [8] compared four URANS models for a Savonius hydro turbine using ANSYS FLUENT, finding Spalart–Allmaras unexpectedly most accurate. However, the study's limitation lies in its narrow model selection.

Table 1 provides a summary of numerical CFD works by different authors. While most of the authors have used k-ε realizable, some use k-w SST. There is a research exploration possibility in using other models, such as k-ε standard wall functions and k-ε enhanced wall treatment (EWT). Which will be validated and used in the paper. Moreover, there is a lack of comparison between Savonius and Darrius turbines at their optimum speed ratios that will be discussed in our paper as well.

Table 1: Work on Drag Based Turbines

Author	**Year**	**Investigation**	**Method**	**Blade Profile**	**Re Number**	**Model**
Mosbahi et al. [9]	2021	Blade shape optimization	3D	Twisted/U-shaped/ Wshaped/ V-shaped semicircular	-	Realizable k-ε
Ramadan et al [10]	2021	Effect of blade profile and deflectors	2D	Semi-circular/modified	1 × 105	Realizable k-ε
Rengma et al. [11]	2023	Blade shape optimization	3D	cubic Bezier curve	1.35 × 10^5	Realizable k-ε
Song et al [12]	2021	Influence of blade shape and wave flume conditions on turbine performance	2D	Semicircular/Benesh/modified Benesh/ elliptical/modified elliptical	-	Realizable k-ε
Shashikumar et al. [13]	2021	Evaluating conventional vs. tapered Savonius turbine designs	3D	Semi-circular	-	SST k-ω
Chaudhari and Shah [14]	2023	Effect of deflector on Savonius turbine incorporating airfoil-shaped blades	3D	NACA6409	2.5 × 105	SST k-ω

For guaranteeing the precision and dependability of CFD simulations of VAWTs for optimization are provided in this section. It addresses fundamental topics such as numerical schemes and algorithms, temporal and spatial discretization, and computational domain size.

Temporal and Spatial Discretization

The reliability of CFD simulations for wind turbines depends heavily on grid quality. High-quality grids improve accuracy and convergence, while poor ones risk errors. Grids are either structured (with orderly quadrilaterals/hexahedra) or unstructured. Structured grids offer easier neighbor access due to their linear layout but are harder to generate for complex geometries [15]. One such example is given in Figure 5 with structured O-grid.

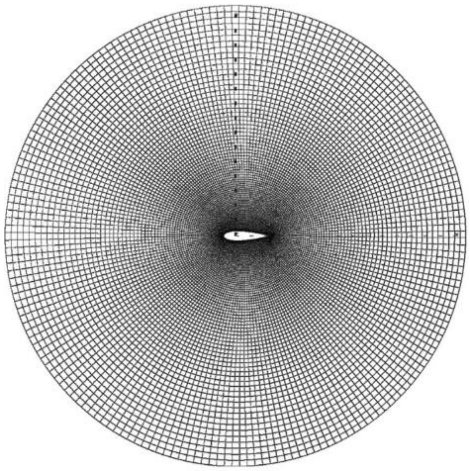

Figure 6: Structured Grid for VAWT [16]

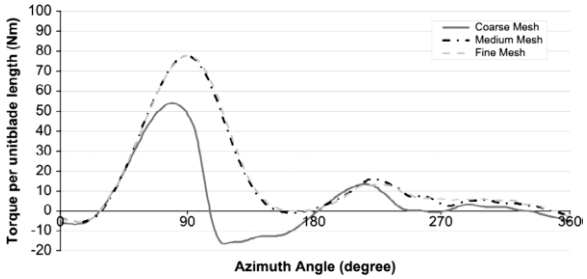

Figure 5: Grid Convergence Study

Grid resolution depends on the problem's complexity, making a grid sensitivity study essential. While finer grids improve accuracy, they also increase computational cost. The optimal grid is found when further refinement shows minimal result changes. Studies often show that medium and fine meshes yield similar results, indicating a medium grid is sufficient. To evaluate grid convergence and calculate discretization errors, Zadeh et al. [17] employed the grid convergence index (GCI) approach as shown in Figure 6. Their study highlights the importance of a grid study, which will be employed in our analysis.

Solvers and domain size

Mach number (M<0.3) for Darrieus wind turbines often indicates that the flow can be considered incompressible, enabling the application of incompressible flow solvers. Under varied operating conditions, Lanzafame et al. [18] evaluated pressure-velocity coupling methods under different conditions, finding PISO most accurate. The COUPLED scheme failed to predict blade flow properly, and SIMPLE performed poorly at low TSRs. Li (2023) [19] analyzed single-blade VAWTs, highlighting their broader application, simpler design, and lower cost. However, accurately predicting wake effects remains challenging. The SIMPLE algorithm performs well at high TSRs but shows slight errors at low speeds, while the COUPLED method deviates more from experimental results. Thus, from the above literature studies SIMPLE algorithm was selected for our analysis. However, these studies did not compare turbulence models for minimizing computational power.

In research on computational domain size, Chen et al. [20] found that torque stays comparatively constant when the computational domain to rotor diameter ratio is greater than 15 as shown in Figure 7. To guarantee full wake formation, the computational domain should be appropriately expanded—ideally up to 14 diameters downstream from the rotor [21]. The computational domain ratio of 20 was suggested by Mohamed [22]. Hence, the above appropriate

domain size was chosen for our CFD analysis on VAWTs. Even if the selection of turbulence model, grid, and domain size is done carefully, an important factor in CFD that should be critically analyzed is studying the tip effects on simulation fidelity. Siddique et al. [23] identified that 2D approximations can overpredict turbine performance by up to 32%, with similar discrepancies observed in other geometric and flow approximations. Hence, it is necessary in our study to compare 2D and 3D models on the basis of accuracy. Another important selection before performing CFD analysis is the turbulence model that is discussed in the section below.

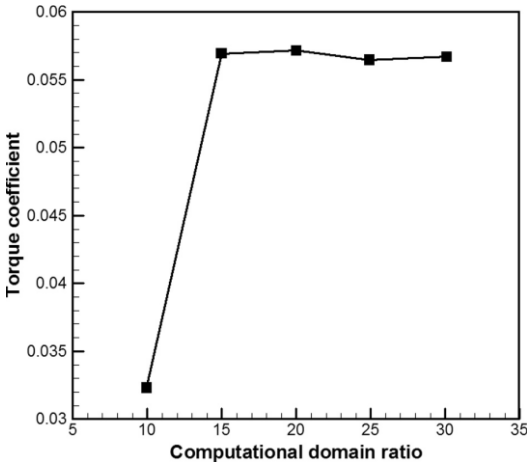

Figure 7: Computational domain size sensitivity study [17]

Turbulence Models:

The RNG k−ϵ model, based on renormalization group theory, improves upon the standard k−ϵ by using variable turbulent Prandtl numbers, accounting for rapid strain, and considering rotation effects, making it more accurate for diverse turbulent flows. For rotating bodies, the realizable k−ϵ model is preferred, as it adjusts Cl based on flow conditions, offering better predictions for swirling and separated flows [24]. The k−ω SST model combines the strengths of k−ω and k−ϵ, using k−ω near walls and gradually transitioning to k−ϵ in the wake and free shear regions [25]. A blending function controls the transition, active near walls, and fading in the wake. The k−ω SST model also includes a modified eddy viscosity to account for shear stress transport, improving accuracy in flows with strong adverse pressure gradients [26]. However, these are all y+ sensitive models, hence there is a need for a computationally inexpensive model which are y+ free.

The Enhanced Wall Treatment (EWT) is a hybrid wall modeling approach that seamlessly blends the viscous sublayer and logarithmic law regions using a damping function, ensuring smooth transitions across varying y+ values. Unlike traditional wall functions, EWT does not impose a strict y+ threshold but instead employs a blending function, Γ, to combine the low-Reynolds-number model for $y^+<6$ and the logarithmic law for $y^+>30$, with a weighted interpolation in the buffer region ($6<y^+<30$). This makes EWT a flexible, grid-independent solution suitable for a wide range of turbulence modeling scenarios in CFD simulations [27]. Hence, EWT will be used in our studies. The gap that this study addresses is the use of computationally inexpensive models such as EWT for VAWT simulation to find optimum TSR for Savonius VAWT and the comparison of Drag-based (Savonius) and Lift-based Darrius turbine's aerodynamic performance while validating results of 2D and 3D CFD analysis against experimental benchmarks.

2. METHODOLOGY

The study validates CFD with experimental data from Blackwell [28]. The study has performed wind tunnel studies of drag-based turbines on various configurations (s/d ratio, Re Number, number of buckets). In our case, we have chosen a 2-bucket rotor with a 4.32 x 10^5 Re Number. 2D and 3D CFD analysis is analyzed and compared. Moreover, a comparison between drag and lift-based turbines is also performed.

Parameter Definitions

The Cp of a turbine is influenced by TSR, which represents the ratio of the rotor blade tip velocity to the freestream velocity of the fluid. This parameter plays a crucial role in determining the efficiency and optimal operating conditions of the turbine.

$$X_\infty = \frac{R\Omega}{V_\infty} \quad (1)$$

Where R is the radius of the turbine, omega is the rotational speed (rad/s), V_∞ is the inlet velocity of the fluid.

An important parameter for evaluating turbine performance is the torque coefficient (Cq). It is defined as the ratio of the torque produced by the turbine rotor to the maximum available torque in the flow. This coefficient helps assess the turbine's ability to convert fluid motion into rotational energy efficiently.

$$\text{Cq} = \frac{Q}{q_\infty R A_S} \quad (2)$$

Where Q is the torque, q_∞ is the dynamic pressure and A_s is the swept area of the turbine.

As air flows past the turbine rotor, its continuity must be maintained, and some energy losses occur during the conversion process. As a result, only a portion of the kinetic energy can be harnessed by the turbine. The efficiency of this energy extraction is represented by the Cp, which is defined as the ratio of the power captured by the turbine to the total available power in the flow. This metric serves as a key indicator of turbine performance.

$$\text{Cp} = \frac{Q\Omega}{q_\infty v_\infty A_5} \quad (3)$$

Where Ω is the rotational speed of the turbine

Cases

The Savonius cases were validated against Maican [5] and Blackwell [28]. Moreover, to compare Savonius performance against Darrius a case study was validated with Siddique et al. [23]. The case studies are shown in Table 2.

Table 2: Validation Cases

Type of VAWT	Case #	Validation case type	Validation parameter w.r.t. C_Q & C_P	Case parameter
Savonius Two-bucket (Drag Type) VAWT	1	2D Static, Maican	5° α, s/d = 0.2	Steady State Validation
	2	3D Static, Blackwell (Run 12)	5° α, s/d=0	Steady State Validation
	3	2D Dynamic, Blackwell (Run 37)	Multiple TSR, s/d = 0.2	(i) Timestep Verification (ii) Mesh Verification (iii) Validation with Experiment
	4	3D Dynamic, Blackwell (Run 37)	Multiple TSR, s/d = 0.2	Validation with Experiment
Darrieus (Lift Type) VAWT	5	2D NACA 0022 Dynamic, Siddique et al	Multiple TSR	Validation with CFD and Darrius and Savonius comparison

In all of the Savonius cases, Re = 4.32 x 10^5 is applied, with Green gauss cell-based gradient and SIMPLE pressure velocity coupling, as it is computationally inexpensive and is found to be accurate in dynamic analysis [23]. A second-order upwind discretization scheme is used for accuracy.

CAD Models

General geometry of the turbine is

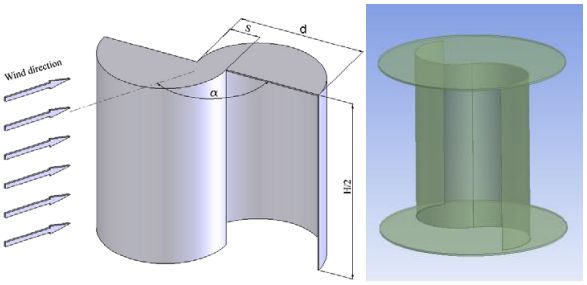

Figure 8: Geometry of Drag Based Turbine

The study analyzes two cases: one with R=0.512m and s/d=0, and the other with R= 0.4512 m and s/d=0.2. Where s is the gap between the blades, R is the radius of the turbine and d is the diameter of the blade

(a) 2D

The sliding mesh technique is employed for dynamic analysis, using an O-type domain with a size 1.1 times the turbine diameter. The computational domain extends 15 m in length, with approximately 12D in the wake region. A highly refined body-fitted mesh is used, ensuring an 8D wake resolution. The domain walls are positioned 5D above and below the turbine. To optimize computational efficiency, the boundary condition at the walls is set as a velocity in the x-direction, avoiding the need to resolve the no-slip condition.

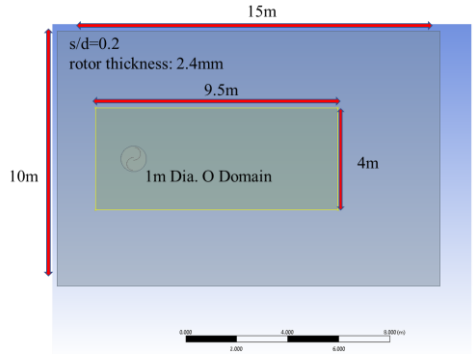

Figure 9: Domain Size of 2D Analysis

(b) 3D

The rotor has a height of 1 meter with a thickness of 2.4 mm. The end plate diameter is set to 1.1 times the rotor diameter, following the approach by Talukdara [29]. Additionally, the end plate thickness is approximated to 5 mm. The geometries for static and dynamic analysis are given below

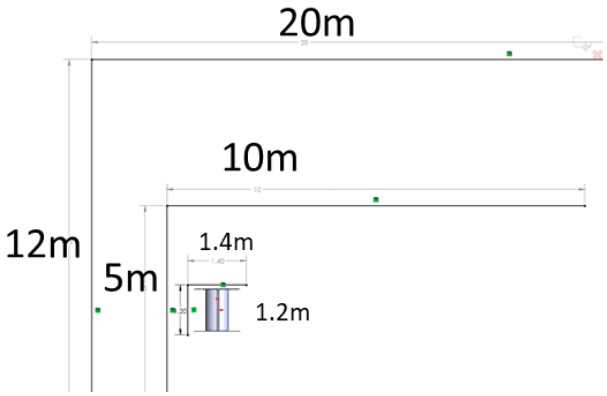

Figure 10: Static Domain of 3D model

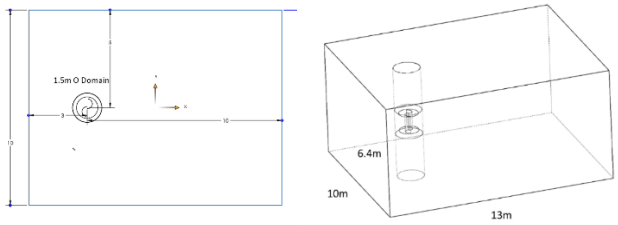

Figure 11: Dynamic domain of 3D model

Computational Domain

(a) 2D

1. Static: y+~=1, k omega, and y+<3 k-ε enhanced wall treatment is used to validate the model
2. Dynamic: To cater all the speed ratios, y+~<3 is taken for k-ε enhanced wall treatment

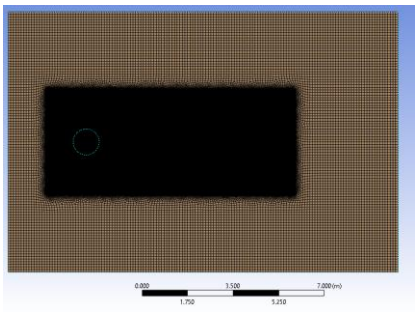

Figure 12: Body Mesh Domain

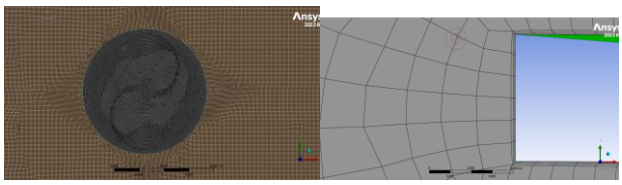

Figure 13: Sliding mesh of 2D Analysis and inflation at blade tip

(b) 3D

Static

The study considers a solidity ratio of s/d = 0, aligning with Run 12 of the Blackwell [28]experiment. The Reynolds number is set at 4.32×10^5, with an angle of attack (AOA) of 5 degrees. The torque coefficient obtained from the simulation is compared against the experimental results to validate the computational model. Tetrahedron Free mesh is used with inflation y+~=1 and k-w SST model having 6 million Elements, here again keeping y+~<3 k-ε enhanced wall treatment model is validated so that it may be applied to the dynamic analysis.

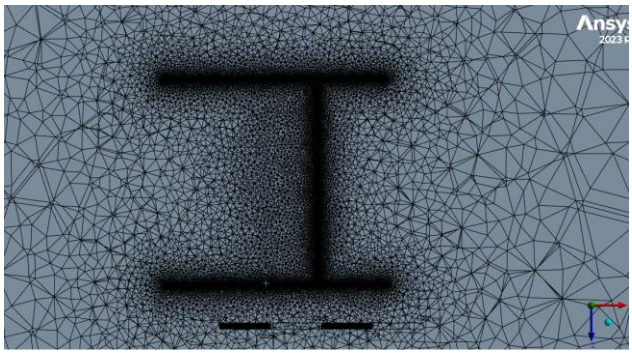

Figure 14: Tetrahedron Mesh of 3D Static Analysis

Dynamic

The Multizone Non-Conformal Sliding Mesh technique is employed for dynamic 3D analysis, ensuring accurate rotor motion simulation. The computational domain consists of approximately 36.04 million elements (36,042,076) to capture the flow details effectively. The k-ε Enhanced Wall Treatment is applied, with inflation layers around the blades to maintain y+ < 3, ensuring proper near-wall resolution for turbulence modeling.

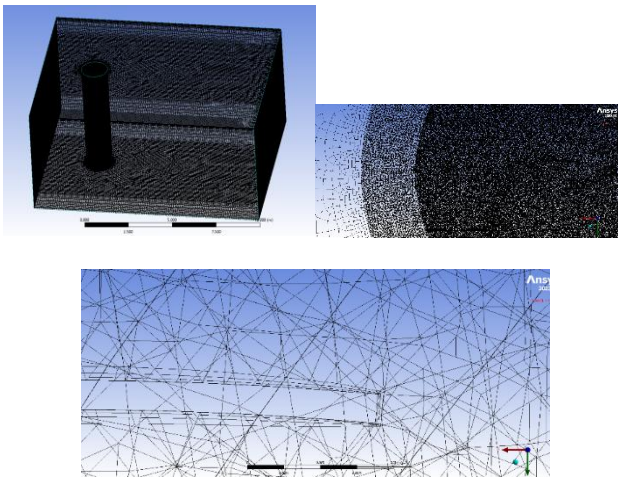

Figure 15: 3D Dynamic Mesh with inflation at blade tip

3. RESULTS AND DISCUSSION

The results are discussed in the following section. The freestream velocity v∞ for Savonius turbine CFD analysis is corrected for wind tunnel blockage using the factor ϵ=0.0162, giving v∞=7(1+0.0162) =7.1134 m/s

(a) Static Analysis

2D Static - Case #1

The 2D geometry analysis includes a comparison of angle and static torque coefficient with the 2D CFD results from Maican and Bris [5]. The computational mesh consists of 80,000 elements, ensuring adequate resolution for the study. Two turbulence models are used: the k-ω SST model with y+ = 0.1 for low Reynolds number modeling and the k-ε EWT with y+ < 3 to validate the model against the k-w SST model

Table 3: Input parameters for static analysis

Angle	Torque	R	As	velocity	Ro	q (Dyn P)
5	2.25443	0.5012	1.0023	7.1134	1.185	29.981

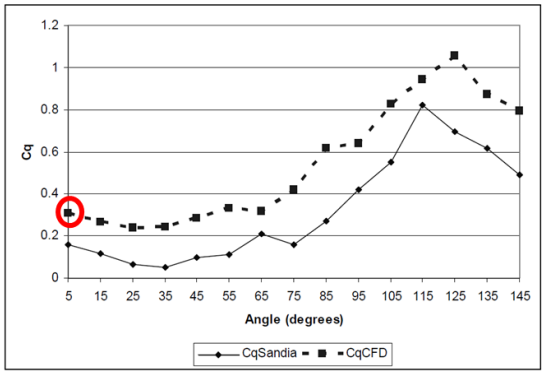

Figure 16: Reference Cq point from Maican [5]

For the 2D numerical analysis, the parameters considered include a spacing ratio (s/d) of 0.2, a Reynolds number (Re) of 4.32×10^5, and an angle of attack (AOA) of 5 degrees. Results are compared for k-w SST and for k-ε enhanced wall treatment:

Table 4: Torque Coefficient comparison for turbulence models

Turbulence Model	CFD (Maican, 2008)	CFD (Present)	Error
K-w SST	0.309	0.318	2.9%
k-ε EWT	0.309	0.316	2.2%

Here, this analysis shows that both models are fairly accurate, showing good comparison with CFD. Here it is noted that the CFD model overpredicts in 2D as it does not capture the turbulence well in 2D, especially in low TSRs, but for now, we can use k-ε enhanced wall function as a turbulence model. This will be validated in the 3D Static analysis as well.

3D Static - Case #2

For the 3D static analysis, the parameters include a spacing ratio (s/d) of 0, a Reynolds number (Re) of 4.32×10^5, and an angle of attack (AOA) of 5 degrees. The mesh is generated using the Tetrahedron Body Meshing Technique, with turbulence models such as K-w SST and K-ε Enhanced Wall Function employed to validate the model for subsequent dynamic analysis. Results are compared in 3D for k-w SST Model and for k-ε EWT.

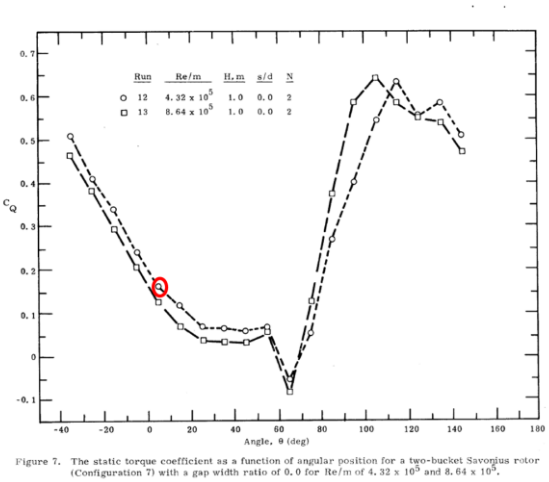

Figure 17: 5 Degree Static Torque Data point from Blackwell [28]

A steady wake forms when air passes through the turbine and a static torque is generated.

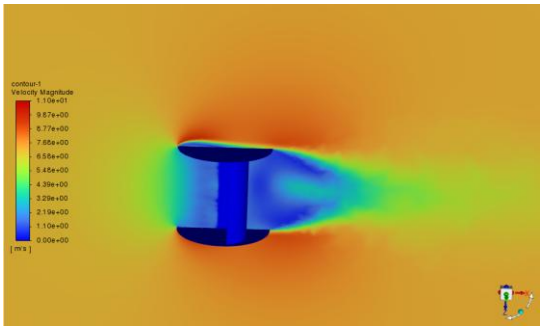

Figure 18: 3D Static Analysis Velocity Contour

Table 5: Torque Coefficient comparison for turbulence models

Turbulence Model	CFD (Maican, 2008)	CFD (Present)	Error (Abs)
K-w SST	0.16	0.1496	0.01
k-ε EWT	0.16	0.1501	0.0099

There is a negligible difference between the two models; hence, the k-ε enhanced wall treatment is recommended for use in dynamic analysis as it is more flexible towards y+.

(b) Dynamic

2D Dynamic – Case #3

For the 2D dynamic validation (Run 37), the spacing ratio (s/d) is 0.2, with a Re of 4.32×10^5. The analysis focuses on the torque coefficient and power coefficient. The inlet velocity, Vin, is set to 7.1134 m/s, with a side wall inlet condition of 7.1134 m/s and a pressure outlet. The turbine's rotational speed is 2.49 rad/s, corresponding to a speed ratio of 0.1586.

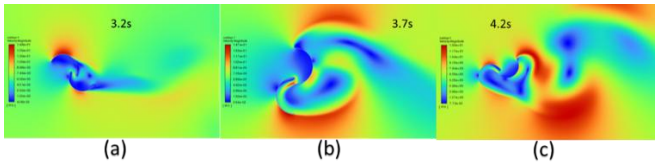

Figure 19: Separation of wake vortices at (a) 3.2s, (b) 3.7s, (c) 4.2s

At a speed ratio of 0.1586, the two crests and troughs complete a full 360° rotation, with maximum torque observed. As the timesteps progress, the solution transitions from transient behavior to a periodic state.

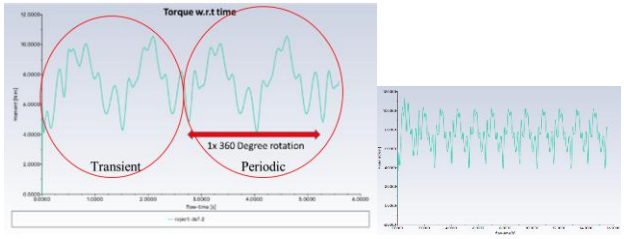

Figure 20: Periodic and Transient Torque Output

At this Reynolds number (4.32×10^5), the periodic behavior typically establishes after 1 second of real flow time.

Mesh Verification/ Independence

The mesh was verified as a standard practice in CFD to ensure accuracy and computational efficiency. Three mesh densities were tested: 0.41 million, 0.55 million, and 0.87 million elements. The percentage error between the 0.55 million and 0.87 million element cases was negligible (0.026%), confirming mesh independence. Based on this verification, 0.55 million elements were selected for the validation study.

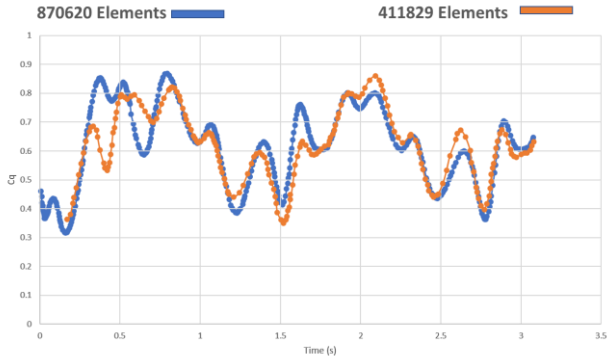

Figure 21: Mesh independence w.r.t Cp results

Table 6: Results of Mesh independence

No of Elements	Parameter	Exp (Blackwell, 1977)	CFD (Average) (Present)	Percentage Error
411829 Elements	Torque Coeff @ 0.1586 Speed Ratio	0.382	0.6201	-
558620 Elements	Torque Coeff @ 0.1586 Speed Ratio	0.382	0.6102	1.596516691
870620 Elements	Torque Coeff @ 0.1586 Speed Ratio	0.382	0.61004	0.026220911

Timestep Verification

The timestep was verified to balance computational expense and accuracy. Three timesteps—0.01, 0.005, and 0.0025—were tested for the 2D dynamic analysis. While all three showed negligible differences, the percentage error between 0.005 and 0.0025 was only 0.003%. This indicated that although 0.01 could be used at 0.1586 TSR, the error would likely increase at higher TSRs. Therefore, 0.005 was selected as the optimal timestep for the analysis.

Table 7 :Timestep verification results for 2D Analysis

Timestep	Parameter	Experiment (Blackwell, 1977)	CFD (Average) (Present)	Percentage Error
0.01	Torque Coeff@ 0.1586 Speed Ratio	0.382	0.61005	-
0.005	Torque Coeff@ 0.1586 Speed Ratio	0.382	0.6102	0.024588149
0.0025	Torque Coeff@ 0.1586 Speed Ratio	0.382	0.61022	0.003277614

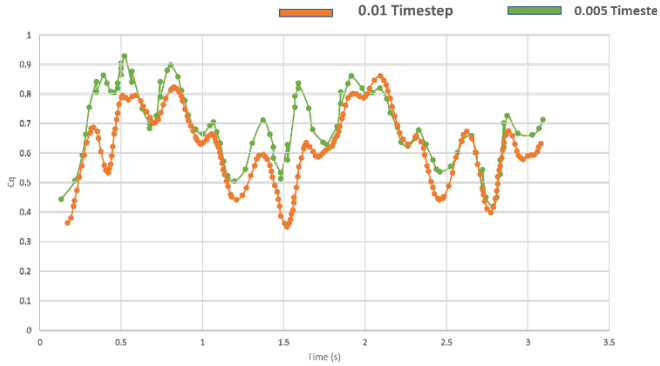

Figure 22: Timestep verification results as coefficient of torque

Another observation is made that the peaks of both results (of timesteps 0.01 and 0.005) follow each other, meaning there is no major change in turbulence and eddies.

Results of 2D Dynamic Analysis

As the flow initiates and the turbine begins to rotate, a series of countercurrent and co-current vortices are generated. At higher tip-speed ratios (TSR), the wake length decreases due to the intensified interaction between the vortices. Wake length is the distance downstream where the flow recovers and returns to its original free-stream velocity.

Table 6: Comparison between High and Low TSRs

Speed Ratio	Parameter	Experiment (Blackwell, 1977)	CFD (Average) (Present)	Abs Error
0.1586	Torque Coeff	0.382	0.61005	0.22805
0.676168	Torque Coeff	0.31739	0.356	0.03861
0.8563	Torque Coeff	0.259489	0.274598	0.015109
1.09	Torque Coeff	0.1846	0.2	0.0154

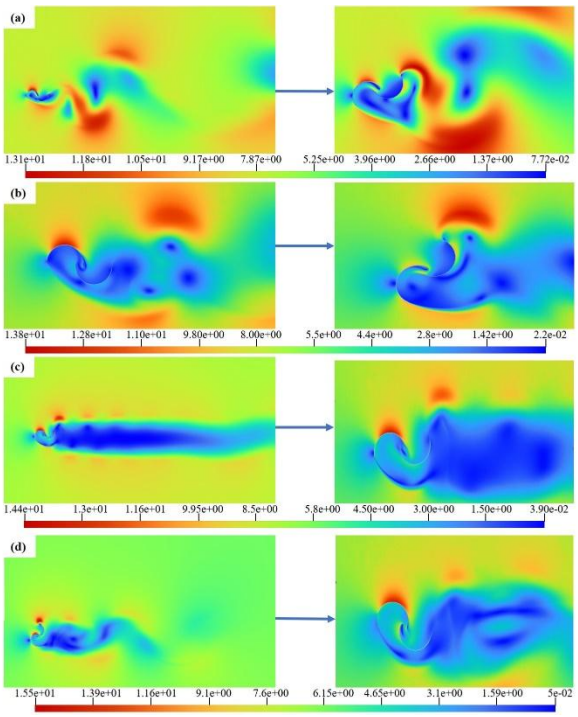

Figure 23 Velocity contours for speed ratio (a) 0.1586 (b) 0.676168 (c) 0.8563 (d) 1.09. Column two represents the zoomed-in view near the rotating domain

As the speed ratio (SR) increases, flow separation occurs later along the blade surface, causing the vortices to move closer together and mix more.

As speed ratio increases rotation decreases the size of the wake in the downstream region. This happens because the rotating body generates a "pumping action," which redirects fluid from the upstream flow into the wake. Since the wake is filled with the pumped fluid earlier, the disturbed region dissipates faster, leading to a shorter wake recovery distance.

Validation (2D Dynamic)

The 2D results were validated against six TSRs in dynamic analysis, showing good agreement with experimental data, with an absolute error below 0.1 and a relative error of approximately 10–15%. However, at a low TSR of 0.1586, the 2D solver overpredicts the results due to high separation effects and low pumping effects, consistent with observations in the literature (Maican and Bris [5]).

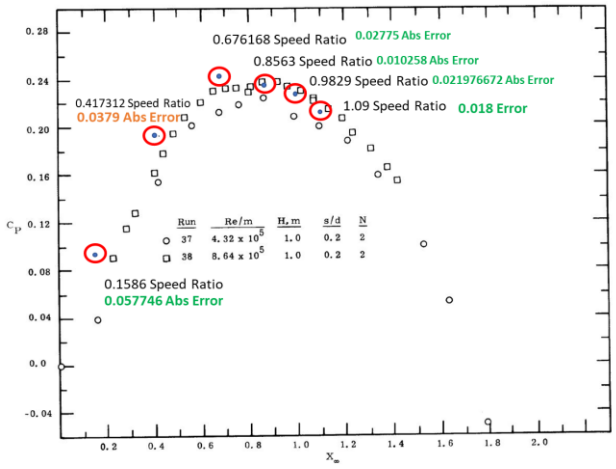

Figure 24: Cp Validation Results comparison with Blackwell [28]

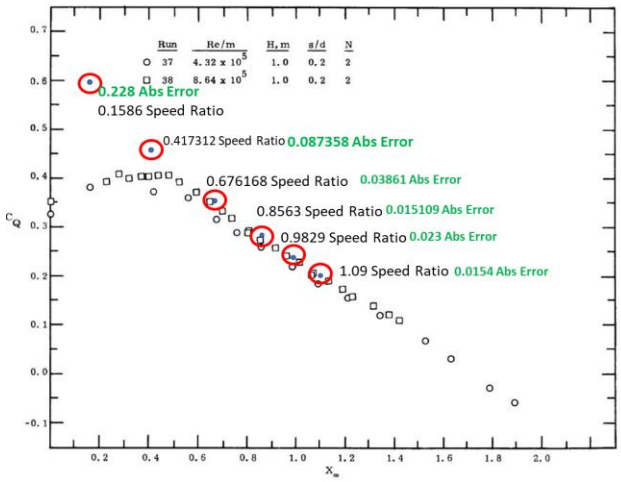

Figure 25: Torque coefficient results validation with Blackwell [28]

High separation effects, resulting from a weak pumping effect, lead to a wake-dominant flow characterized by turbulence-induced torque fluctuations. These fluctuations manifest as ripples in the torque curve at low tip-speed ratios (TSR), whereas at higher TSRs, the increased pumping effect stabilizes the wake, resulting in a smoother torque response.

Table 9: Torque and Power coefficient results validation with Blackwell (1977) [28]

TSR	C_P CFD	C_P Exp.	C_Q CFD	C_Q Exp.	C_Q Error (%)
0.1586	0.09675	0.03900	0.61000	0.38200	59.69%
0.4173	0.19246	0.15451	0.46120	0.37384	23.35%
0.6762	0.24072	0.21296	0.35600	0.31739	12.14%
0.8563	0.23514	0.22488	0.27460	0.25949	5.82%
0.98295	0.23198	0.21000	0.23600	0.21300	10.80%
1.0900	0.21800	0.20000	0.20000	0.18460	8.34%

Additionally, 2D simulations tend to overpredict separation effects, leading to relatively higher errors at lower TSRs. As the pumping effect strengthens with high TSRs, fluctuations diminish, and turbine torque stabilizes. This instability at low TSRs may contribute to turbine vibrations due to torque variations**.** Furthermore, simulations indicate that maximum torque is achieved at an intermediate TSR. At low TSRs like 0.1586, the wake extends sideways, causing fluctuations in the torque coefficient, whereas at higher TSRs, the wake remains more confined behind the turbine, improving stability and performance. But at extreme TSRs (1.01 TSR) the torque coefficient has less ripples like the intermediate TSR (0.676), but Torque decreases overall.

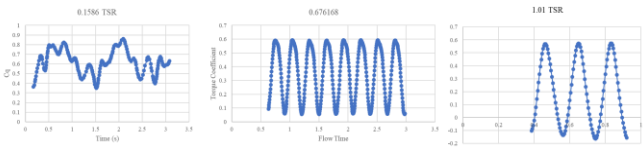

Figure 26: Torque Ripples of TSR 0.1586 (left), 0.676 (middle) ,and 1.01 (right) comparison

The results show that the ideal TSR for a wind turbine is 0.676 with 0.24 Power coefficient.

3D Dynamic Validation – Case#4

The 3D numerical analysis was conducted using a s/d) of 0.2 and a Re of 4.32×10^5. The k-ε EWT turbulence model was employed for accurate near-wall flow resolution. The boundary conditions included an inlet velocity of 7.1134 m/s, with the same velocity applied at the sidewall inlet to maintain consistency. A pressure

outlet condition was used at the domain exit. The turbine operated at a rotational speed of 2.49 rad/s, corresponding to a TSR of 0.1586.

Table 10: Torque Coefficient Validation Results

Parameter	Exp (Blackwell, 1977)	CFD (Average) (Present)	Abs Error
Torque Coeff @ 0.1586 Speed Ratio	0.382	0.365	0.017
Torque Coeff @ 0.417312 Speed Ratio	0.373842	0.3414	0.032

There is only 4% Deviation from experimental results with absolute error = 0.017, hence our model is validated, even at high TSR the absolute error is only 0.032.

The streamline and pressure distribution graphs indicate that the flow begins to exhibit a pumping effect at low TSR, though it remains relatively weak. The pressure plot further highlights that the turbine's cups, when facing the incoming flow, generate the necessary drag to produce torque, facilitating the turbine's rotation.

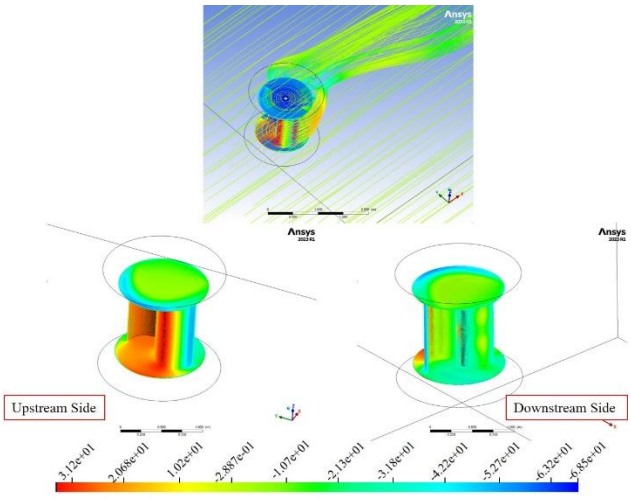

Figure 27: Streamline and Pressure Plots

The 3D velocity contours illustrate that the wake is well captured across the two TSRs. As TSR increases, turbulence intensity also rises, leading to enhanced wake vortex mixing and forming patterns characteristic of real turbulent flows. However, at higher TSRs, the error begins to accumulate due to the increased turbulence intensity. This necessitates a more refined computational domain to accurately capture the flow dynamics, as the RANS model, being inherently dissipative, tends to smooth out smaller turbulence structures.

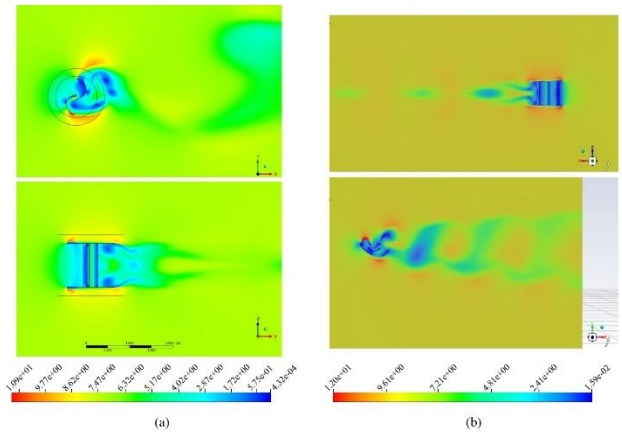

Figure 28: Velocity contour comparison with TSRs

In 3D simulations, the results closely match experimental data even at low TSRs, demonstrating improved accuracy compared to 2D models. Using the same turbulence model and y+ range, the 3D approach effectively reduces torque ripples, which are overpredicted in 2D due to its limitations in capturing complex separation effects. Additionally, true turbulence dynamics are inherently three-dimensional, further reinforcing the reliability of 3D simulations in representing realistic flow behavior around the turbine.

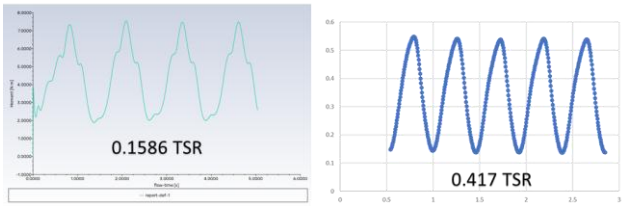

Figure 29: Torque Ripple comparison with TSRs

As discussed in the 2D analysis, low TSRs exhibit torque fluctuations due to high separation

effects. However, since 2D tends to overpredict at low TSRs with high separation and low pumping effects, the 3D results at 0.1586 TSR show only minor fluctuations, aligning closely with experimental data with just a 4% error. Furthermore, these findings confirm that the k-ε enhanced wall treatment effectively captures flow dynamics, providing a validated framework for applying optimization techniques in future studies.

Comparison with Lift-Based (Darrius Turbine) – Case#5

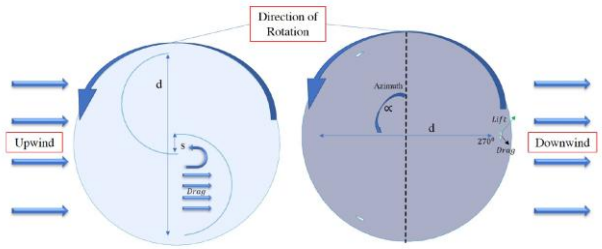

Figure 30: Savonius (Left) and Darrius (Right) schematic

The performance of Savonius and Darrius turbines is compared. For comparison, a study of Siddique et al. [23] was taken as a Lift-based (Darrius) benchmark. The Reynolds number is around 4×10^5. The study was first validated at TSR=3.0. The results matched closely with under 5% error as shown in Figure 28.

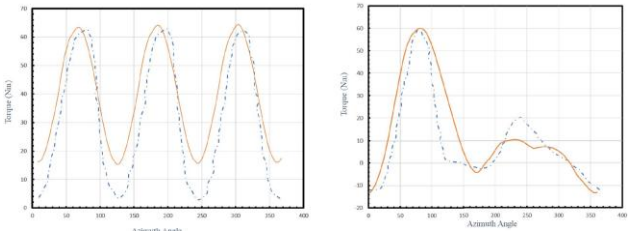

Figure 31: Overall (Left) and blade torque (Right) comparison w.r.t Azimuth angle of CFD present (Solid)

After validation of our CFD model, the comparative analysis was done for the Savonius turbine with Darrius to analyze their optimum working conditions. Hence, a TSR sweep was performed to compare both turbines as shown in Figure 29. The analysis confirms that the Darrius is optimum at TSR 3.0, which is higher than the optimum TSR of Savonius, which is at 0.676. Moreover, the Darrius outperforms Savonius by 122%. This analysis shows that even though Lift-based turbines have poor self-startup and no performance in low TSRs, they outperform Drag-based turbines at high TSRs. However, the ability of Drag-based turbines to perform well under low TSR conditions show that these turbines can be used in low wind speed conditions for power output.

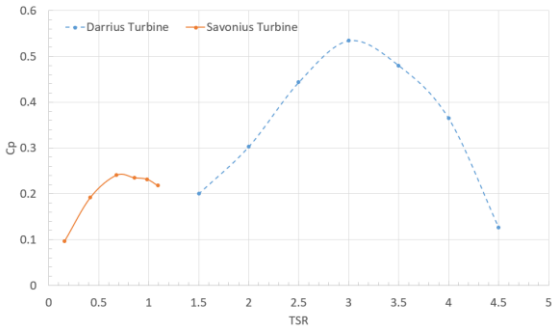

Figure 32: Comparison of Darrius (dashed) with Savonius (solid) Cp

4. CONCLUSION

This study analyzed the aerodynamic performance of a drag-based Savonius VAWT using CFD to determine the optimal TSR. The study reveals that for a given Reynolds number of 4.32×10^5, the ideal TSR is 0.676, which yields a maximum Cp of 0.24. The results show that Cp initially increases from 0.1586 TSR, reaching peak performance at 0.676 TSR, before beginning to decline. This trend underscores the balance between aerodynamic efficiency and wake dynamics, where excessive TSR values lead to increased turbulence and energy dissipation, which ultimately reduces overall performance.

The analysis of wake characteristics, including wake size and length, demonstrated that higher

TSR values reduce the wake length due to stronger rotational effects and better mixing of vortices. Both 2D and 3D models were used for numerical analysis, and key trends were validated against experimental data [28]. The findings emphasize the importance of selecting an optimal TSR to maximize power and torque coefficients while minimizing wake losses. Furthermore, the study highlighted the role of turbulence modelling techniques, such as the k-ε enhanced wall treatment, in accurately capturing near-wall effects. The results suggest that the choice of TSR significantly impacts turbine performance, and although 3D model which is a high-fidelity model, provides very accurate results for optimization and to see the pattern of Cp 2D analysis can be used, which is fairly accurate, 10% at intermediate TSRs. Moreover, the comparison between Lift and Drag-based turbines shows that even though Lift-based turbines perform well in high TSR conditions, the Drag-based turbines perform well in low wind conditions; hence, these can be used in domestic and urban areas, as they also would have better self-startup (at low TSR).

Future research should focus on applying optimization algorithms like multivariable Bayesian Optimization [30] to refine TSR selection and improve turbine geometry. This would lead to enhanced efficiency and stability of VAWTs in real-world applications.

5. ACKNOWLEDGMENTS

The authors would like to express their sincere gratitude to Dr. Haris Moazzam Sheikh from the University of Southampton for his valuable input and guidance. Their insights and encouragement have been instrumental in shaping this research.

6. REFERENCES

[1] M. Ghasemian and A. Nejat, "Aerodynamic noise prediction of a horizontal Axis wind turbine using improved delayed detached eddy simulation and acoustic analogy," *Energy Convers Manage,* p. 99:210–20, 2015.

[2] S. Gumuła, T. Knap, P. Strzelczyk and Z. Szczerba, "Wind Energy," 2006.

[3] A. Chaudhuri, R. Datta, M. Kumar, J. P. Davim and S. & Pramanik, "Energy conversion strategies for wind energy system," *Electrical, mechanical and material aspects,* vol. 15, no. 3, p. 1232.

[4] B. Hand, G. Kelly and A. & Cashman, "Aerodynamic design and performance parameters of a lift-type vertical axis wind turbine," *A comprehensive review. Renewable and Sustainable Energy Reviews,* vol. 110699, p. 139, 2021.

[5] E. Maican and a. S.-S. Biris, "Comparative Analysis of a Wind Turbine's Performances by Means of CFD Simulations," *J. Agric. Mach. Sci. (Journal of Agricultural Machinery Science),* vol. 4, no. 2, p. 247–252, 2008.

[6] G. Ferrari, D. Federici, P. Schito, F. Inzoli and R. Mereu, "CFD study of Savonius wind turbine: 3D model validation and parametric analysis," *Renewable Energy,* 2017.

[7] A. Dewan, S. Tomar, A. Bishnoi and T. Singh, "Computational fluid dynamics and turbulence modelling in various blades of Savonius turbines for wind and hydro energy: Progress and perspectives," *Ocean Engineering,* vol. 283, 2023.

[8] A. Heydari, A. Mohammadi, A. Nabhani and A. Mohammadi, "CFD Simulation of Savonius Cross-flow Hydrokinetic Turbine Using Various URANS Turbulence Models," *World Congress on Civil, Structural, and Environmental Engineering,* 2024.

[9] M. Mosbahi, M. Lajnef, M. Derbel, B. Mosbahi, Z. Driss, C. Aricò and a. T. Tucciarelli, "Performance improvement of a Savonius water rotor with novel blade shapes," *Ocean Engineering,* vol. 237, p. 109611, 2021.

[10] A. Ramadan, M. Hemida, W. Abdel-Fadeel, W. Aissa and a. M. Mohamed, ""Comprehensive experimental and numerical assessment of a drag turbine for river hydrokinetic energy conversion," *Ocean Engineering,* vol. 227, p. 108587, 2021.

[11] T. S. Rengma, M. K. Gupta and a. P. Subbarao, "A novel method of optimizing the Savonius hydrokinetic turbine blades," *Renewable Energy,* p. 119091, 2023.

[12] R. Song, Y. Wu, Z. Lin, C. Ren and a. S. Fang, "Study on the influence of blade profile on hydraulic Savonius turbine under wave action," *Ocean Engineering,* vol. 240, p. 109863, 2021.

[13] C. Shashikumar, H. Vijaykumar and a. M. Vasudeva, "Numerical investigation of conventional and tapered Savonius hydrokinetic turbines for low-velocity hydropower application in an irrigation channel," *Sustainable Energy Technologies and Assessments,* vol. 43, p. 100871, 2021.

[14] V. N. Chaudhari and S. P. S. b, "Numerical investigation on the performance of an innovative Airfoil-Bladed Savonius Hydrokinetic Turbine (ABSHKT) with deflector," *International Journal of Thermofluids,* vol. 17, p. 100279, 2023.

[15] J. Blazek, Computational fluid dynamics: principles and applications., Elsevier Ltd;, 2015.

[16] P. Kozak, D. Vallverdu and D. & Rempfer, "Modeling vertical-axis wind turbine performance:Blade element method vs. finite volume approach.," in *12th International Energy Conversion Engineering Conference*, (IECEC 2014).

[17] S. N. Zadeh, M. Komeili and M. Paraschivoiu, "Mesh convergence study for 2-D straight-blade vertical axis wind turbine simulations and estimation for 3-D simulations," *Transactions of The Canadian Society for Mechanical Engineering ,* vol. 38, p. 487–504, 2014.

[18] R. Lanzafame, S. Mauro and M. Messina, "2D CFD Modeling of H-Darrieus Wind Turbines Using a Transition Turbulence Model," *Energy Procedia,* vol. 45, p. 131–140, 2014.

[19] Y. Li, S. Yang, F. Feng and K. Tagawa, "A review on numerical simulation based on CFD technology of aerodynamic characteristics of straight-bladed vertical axis wind turbines.," *Energy Reports,* vol. 9, p. 4360–4379., 2023.

[20] J. Chen, L. Chen, H. Xu, H. Yang, C. Ye and D. Liu, "Performance improvement of a vertical axis wind turbine by comprehensive assessment of an airfoil family," *Energy,* vol. 114, p. 318–31, 2016.

[21] M. R. Castelli, G. Ardizzon, L. Battisti and E. Benini, "Modeling Strategy and Numerical Validation for a Darrieus Vertical Axis Micro-Wind Turbine," *ASME 2010 International Mechanical Engineering Congress and Exposition,* pp. 1-10, 2010.

[22] M. Mohamed, "Performance investigation of H-rotor Darrieus turbine with new airfoil shapes.," *Energy,* vol. 47, p. 522–30, 2012.

[23] M. S. Siddiqui, N. Durrani and I. & Akhtar, "Quantification of the effects of geometric approximations on the performance of a

vertical axis wind turbine," *Renewable Energy,* vol. 74, p. 661–670, 2015.

[24] S. Orszag, V. Yakhot, W. Flannery and F. Boysan, "Renormalization group modeling and turbulence simulations," *Near-Wall Turbulent Flows,* p. 1031–1046, 1993.

[25] F. Menter, "Two-equation eddy-eiscosity turbulence models for engineering applications," *AIAA Journal,* vol. 32, p. 1598–605, 1994.

[26] D. Johnson and L. King, "A mathematically simple turbulence closure model for attached and separated turbulent boundary layers," *AIAA Journal,* vol. 23, p. 1684–92., 1985.

[27] A. U. GUIDE, "Enhanced Wall Treatment," ANSYS Inc., 2009. [Online]. Available: https://www.afs.enea.it/project/neptunius/docs/fluent/html/th/node101.htm.

[28] B. F. Blackwell, R. E. Sheldahl and L. V. Feltz, "Wind Tunnel Performance Data for TWO- and Three-Bucket Savonius Rotors," *Sand,a Laboratories, Albuquerque,* 1977.

[29] P. K. Talukdara, A. Sardarb, V. Kulkarnia and U. K. Sahaa, "Parametric analysis of model Savonius hydrokinetic turbines through experimental and computational investigations," *Energy Conversion and Management,* 2018.

[30] Z. Vangelatos, H. M. Sheikh, P. S. Marcus, C. P. Grigoropoulos, V. Z. Lopez, G. Flamourakis and M. & Farsari, "Strength through defects: A novel Bayesian approach for the optimization of architected materials," *Science Advances,* vol. 9, no. 34, p. 4438, 2023.

[31] K. Pytel, "Educational, Economic, and Environmental Impacts of Wind Energy Resource," WNUP: Krakow, Poland, 2022.

[32] M. Ghasemian, Z. Najafian Ashrafi and A. (. & Sedaghat, "A review on computational fluid dynamic simulation techniques for Darrieus vertical axis wind turbines.," *Energy Conversion and Management,* vol. 149, pp. 87-100, 2017.

[33] M. Basumatary, A. Biswas and a. R. D. Misra, "CFD study of a combined lift and drag-based novel Savonius vertical axis water turbine," *J. Mar. Sci. Technol.,* vol. 27, 2022.

[34] P. Bachant, M. Wosnik, B. Gunawan and V. S. & Neary, "Experimental study of a reference model vertical-axis cross-flow turbine," *PLoS ONE,* vol. 11, no. 9, 2016.

[35] S. Aurélien and J. & Peters, "Gradient-based optimization methods for CFD.," *Journal of Computational Fluid Dynamics,* vol. 20, no. 4, pp. 567-589, 2020.

[36] D. E. Goldberg, Genetic Algorithms in Search, Optimization, and Machine Learning, Addison-Wesley, 1989.

[37] S. Kirkpatrick, C. D. Gelatt and M. P. & Vecchi, "Optimization by Simulated Annealing.," *Science,* vol. 220, no. 4598, pp. 671-680, 1983.

[38] A. Rezaeiha, I. Kalkman and B. Blocken, "CFD simulation of a vertical axis wind turbine operating at a moderate tip speed ratio: guidelines for minimum domain size and azimuthal increment.," *Renewable Energy,* vol. 107, p. 373–85., 2017.

[39] O. Verhoeven, "Trailing Edge Noise Simulations: Using IDDES in OpenFOAM.,"

Master's Thesis, Delft University of Technology., 2011.

[40] J. Leishman, " J. Gordon Leishman," 2nd ed. ed., Cambridge University Press, 2006.

[41] E. Jacobs and A. Sherman, "Airfoil section characteristics as affected by variations of the Reynolds number," *Tech. rep Washington. D.C: National Advisory Committee for Aeronautics,* 1937.

[42] D. A. I. J. Forrester, D. A. Sóbester and P. A. J. Keane, Engineering Design via Surrogate Modelling: A Practical Guide, Wiley., 2009.